Journal of Theoretical and Applied Mechanics, Sofia, 2011, vol. 41, No. 1, pp. 33–50

DYNAMIC ANALYSIS OF HELICAL GEARS SUPPORTED BY ROLLING ELEMENT BEARINGS

Mohamed Slim Abbes, Taissir Hentati, Mohamed Maatar,
Tahar Fakhfakh, Mohamed Haddar
Dynamics of Mechanical Systems Research Unit,
Mechanical Engineering Department,
National Engineering School of Sfax, BP 1173, 3038 Sfax, Tunisia University,
e-mails: ms_abbes@yahoo.fr, taissirhentati@yahoo.fr

[Received 15 November 2010. Accepted 28 February 2011]

Abstract. This paper presents a simulation model for gear and bearing interactions in the presence of faults. A global model predicting dynamical behavior of a gear supported by four angular ball bearing system is developed, based on finite element approach. The implemented model has the capacity of considering gear transmission error and ball bearing waviness as sources of excitation in terms of forces or imposed displacements. The Hertzian contact theory is applied to calculate the elastic deflection and the non linear contact force exerted by the totality bearings balls on the input and output shafts. The nonlinear differential equations are iteratively resolved using the Newmark integration technique coupled with the Newton Raphson method. The influence of the Ball bearing waviness order on the system transmission dynamic behaviour is studied. The results show the presence of system characteristic frequencies and their harmonics, and also, the frequencies resulting from waviness, which change with order and type of imperfection.
Key words: angular ball bearing, gear mesh, dynamic analysis, waviness.

1. Introduction

The prediction and control of ball bearing dynamic behaviour are becoming, over the years, some of the major concerns in rotating machinery design. Rotating contact ball bearings, as one sources of internal excitation, have attracted an important interest because of the nonlinear Hertzian contact forces, which generate vibrations and noise. The generated vibrations coupled with additional defect excitation, such as the waviness of the inner and outer

races, become more pronounced and can cause catastrophic machine element failure. Thus, it is necessary to develop models to simulate the dynamic behaviour of the whole machine systems, where defects can be implemented under different operating conditions. Several studies have been extensive literature on this point and in particular, a remarkable diversity of mathematical models as discussed by Lim T. C. and Singh R. [1, 2]. They suggested an analytical approach based on the determination of a stiffness matrix associated to five degrees of freedom of the inner race in its relative movement with respect to the outer race. The proposed matrix includes the beam flexion and housing coupling for the two types of rolling bearings (ball and roller).

Jang G. and Jeang S. W. [3, 4] present an analytical model to investigate vibration due to ball bearing waviness in a rotating system. The centrifugal force gyroscopic moment and the waviness of the ball are included in the kinematics constraints and the force equilibrium equations.

Harsha S. P. [5] theoretically studied the effects of rotor speed with geometrical imperfections. The author presents an analytical model for investigating structural vibrations of a high-speed rotor supported by rolling bearings. The results show the manifestation of instability and chaos in the dynamic behaviour as the speed of the rotor-bearing system is modified.

Kankar *et al.* [6] presented a theoretical model to analyze the effect of distributed defects on the vibration characteristics of a rotor bearing system by considering a two-degree of freedom system (dofs). The conclusion of this work shows that nonlinear dynamic responses are attributed to large internal radial clearance, distributed defects and ball waviness.

Rafsanjani *et al.* [7] proposed an analytical model to study the nonlinear dynamic behaviour of rolling element bearing systems including surface defects. In this model, various surface defects due to local imperfections on raceways and rolling elements are considered.

Sawalhi N. and Randall R. B. [8] presented a combined gear/bearing dynamic model for a gearbox test rig to study the interaction between gears and defect bearings. A lumped mass parameter model of 34-dofs is considered for this study.

Abbes M. S. *et al.* [9] simulated the vibration and the noise radiation of a single-stage gearbox associated with the changing stiffness of the meshing teeth and the effect of the fluid inside the gearbox housing is considered. Numerical simulations have been carried out to investigate the effects of the gear mesh stiffness fluctuation on the dynamic response of the coupled system. They showed that the vibration responses are significantly modified by considering the cavity fluid effect. The acoustic field depends on the resonance

frequencies of the whole gearbox.

Walha L. *et al.* [10] analyzed the vibrations of a two-stage gear system with mesh stiffness fluctuation, bearing flexibility and backlash. The proposed 12-dofs model consists of a two-stage spur gear, three shafts, and two inertias representing load and prime mover and three bearings. The conclusion of this work shows that the dynamic behaviour of such structure is characterized by its complexity which comes mainly from the coupling between the periodic meshes stiffness fluctuations with the presence of backlashes between teeth. Few studies were interested in the influence of the gearbox ball bearing systems on its dynamic behaviour. The gear and bearing interactions in the presence of faults is always neglected and the vibratory responses are usually computed by considering only the effect gear transmission error.

The objective of this work presented in this paper is to perform a theoretical investigation for studying the dynamic behaviour of helical gears supported by defect element bearings. A global model predicting dynamical behaviour of a gear-coupled two shaft bearing system is developed based on the finite element approach. The gear-meshing phenomenon is modelled as a gear stiffness matrix deduced from gears geometrical characteristics and the instantaneous gear contact length. The Hertzian contact theory is applied to calculate the elastic deflection and the non linear contact force exerted by the totality bearings balls on the input and output shafts. The developed model is derived to observe the effect of the internal excitation sources such as the gear mesh stiffness fluctuation and the ball bearing waviness on the vibration characteristics of the machine elements.

2. Ball Bearing Model

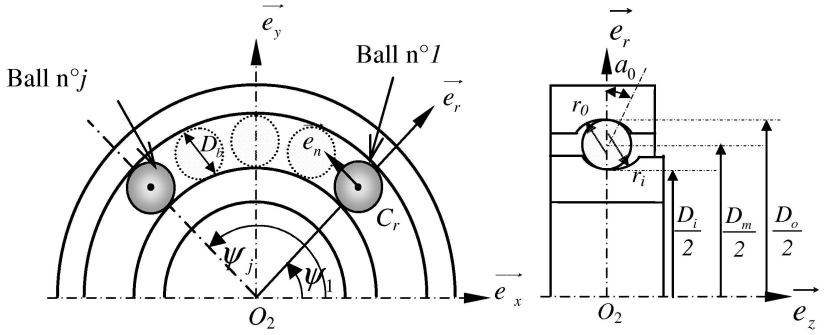

Fig. 1. Coordinate systems of a ball bearing

The dynamic behaviour of a rotor application can be influenced by the design of the ball bearing. The most important components of a ball bearing presented in Fig. 1 are the inner race, the cage, the outer race and the rolling elements. We note the ball diameter D_b, the pitch diameter D_m, the outer and inner raceway groove diameters D_o and D_i, the rolling elements number Z, and the unloaded contact angle α_0 [11].

Two coordinate systems, shown in Fig. 1, are considered. $\Re_1$ represents outer race co-ordinate system, where (x, y, z, θ_x, θ_y) corresponds to the degrees of freedom of the inner race centre. $\Re_2$ is a local cage coordinate system, having the origin at an initial rolling element centre C_r. The outer race centre O_1 is assumed to be fixed in the global frame $\Re_1$. The degree of freedom θ_z is null corresponding to the bearing axis rotation.

2.1. Surface waviness

Even if the geometry of a ball bearing is perfect, it may produce vibration. The contact surfaces of the ball and racing guide always deviate from their perfect form [12], as a result of imperfections in the Ball bearing manufacturing process.

Waviness is a typical defect produced by these manufacturing processes and consists of sinusoidal shaped imperfections on the contact surface of the bearing components (Fig. 2). Waviness imperfections produce important vibrations which can be transmit, from the dynamic to the static part of the rotating machine. The magnitudes of these variations depend on the amplitude of the imperfection.

The following equations can represent respectively the radial and the

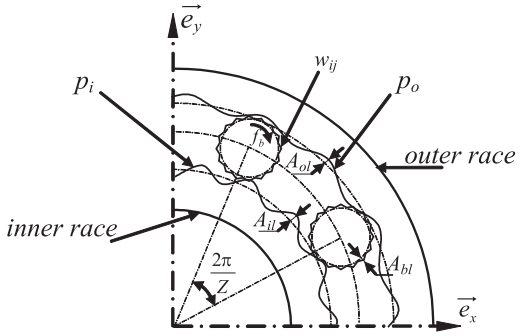

Fig. 2. Inner race, outer race and ball waviness

axial waviness of the inner and outer race, p_{ij}, p_{oj}, q_{ij} and q_{oj} [4]:

$$p_{oj} = A_{ol}\cos\left[-l\left(\omega_o - \omega_c\right)t + \frac{2\pi l}{Z}\left(j-1\right) + \alpha_{ol}\right], \tag{1}$$

$$p_{ij} = A_{il}\cos\left[-l\left(\omega_i - \omega_c\right)t + \frac{2\pi l}{Z}\left(j-1\right) + \alpha_{il}\right], \tag{2}$$

$$q_{oj} = B_{ol}\cos\left[-l\left(\omega_o - \omega_c\right)t+, \frac{2\pi l}{Z}\left(j-1\right) + \beta_{ol}\right], \tag{3}$$

$$q_{ij} = B_{il}\cos\left[-l\left(\omega_i - \omega_c\right)t + \frac{2\pi l}{Z}\left(j-1\right) + \beta_{il}\right]. \tag{4}$$

In the above equations, l, ω_c, ω_o and ω_i are the waviness order, the cage, outer race, and inner race rotating frequencies respectively.

A_{ol}, A_{il}, B_{ol}, B_{il} and α_{ol}, α_{il}, β_{ol}, β_{il} are the amplitudes and initial phase angles of the inner and outer race in contact with the j^{th} ball respectively.

The phase angle of ball waviness in contact with the outer race is 180 °C ahead of the ball waviness in contact with the inner race, so that the ball waviness in contact with the inner and outer race is given as [4]:

$$w_j = A_{bl}\left[\cos\left(l\omega_b\, t + \alpha_b^l\right) + \cos\left(l\omega_b\left(t + \frac{\pi}{\omega_b}\right) + \alpha_b^l\right)\right], \tag{5}$$

with, A_{bl} and α_b^l are the ball waviness amplitude and initial phase.

$\omega_b$represents the ball rotating frequency.

2.2. Forces exerted by defected angular ball bearing

The external load generates inner race centre translation $u_2^{\Re_1}(O_2)$ and angular displacements $\Omega_2^{\Re_1}(O_2)$ in the global frame. They are written as:

$$u_2^{\Re_1}(O_2) = \left\{\begin{array}{c} x \\ y \\ z \end{array}\right\}_{\Re_1} \quad \text{and} \quad \Omega_2^{\Re_1}(O_2) = \left\{\begin{array}{c} \theta_x \\ \theta_y \\ 0 \end{array}\right\}_{\Re_1}. \tag{6}$$

An elastic deformation of the j^{th} rolling element occurs under the effect of external loading. It is defined as the total interaction following the normal direction and it can be expressed as [2]:

$$\Delta_j = d\left(\psi_j\right) - d_0 = \sqrt{\overset{*}{\Delta}{}_{rj}^2 + \overset{*}{\Delta}{}_{zj}^2} - d_0 - w_j, \tag{7}$$

where $d(\psi_j)$ and d_0 are, respectively, the loaded and the unloaded relative distance between the inner and the outer raceway groove curvature centres O_{1j} and O_{2j}, and $\overset{*}{\Delta}_{rj}$, $\overset{*}{\Delta}_{zj}$ are the radial and axial elastic deformations. Introducing the waviness expressions (1–5), the radial and axial elastic deformations can be written as [4]:

$$(8)\quad \begin{cases} \overset{*}{\Delta}_{rj} = x\cos\psi_j + y\sin\psi_j - (a_i + q_{ij}) \times (\theta_x \sin\psi_j - \theta_y \cos\psi_j) \\ \qquad\qquad +d_0\cos\alpha_0 + p_{ij} - p_{oj} \\ \overset{*}{\Delta}_{zj} = z + z_p + (R_i + p_{ij})(\theta_x \sin\psi_j - \theta_y \cos\psi_j) + d_0\sin\alpha_0 + q_{ij} - q_{oj} \end{cases}.$$

A negative elastic deformation indicates no contact between ball and the two races. In this case the elastic deformation is null. The loaded contact angles between rolling element – inner race and rolling element – outer race are the same, when centrifugal forces are neglected. The loaded contact angle α_j is given:

$$(9)\qquad \tan\alpha_j = \frac{\overset{*}{\Delta}_{zj}}{\overset{*}{\Delta}_{rj}}.$$

The ball races contact can be computed from the classical Hertz point – contact theory for a positive elastic deformation. The forces exerted by the totality rolling elements on the inner race are computed by:

$$(10)\quad \sum \vec{F}_{pal} = \begin{cases} \sum_{j=1}^{Z} -Kp\Delta_j^{1,5} \cdot \begin{Bmatrix} \cos\alpha_j \cos\psi_j \\ \cos\alpha_j \sin\psi_j \\ \sin\alpha_j \end{Bmatrix}_{R_1} \\ \sum_{j=1}^{Z} -Kp\Delta_j^{1,5} \begin{Bmatrix} R_1 \sin\alpha_j \sin\psi_j - a_1 \cos\alpha_j \sin\psi_j \\ -R_1 \sin\alpha_j \cos\psi_j + a_1 \cos\alpha_j \cos\psi_j \end{Bmatrix}_{R_1} \end{cases},$$

where Kp represent the Hertz constant.

3. Finite element modelling of gear transmission system

The presented model allows studying the dynamic behaviour of a rotor dynamic application containing ball bearings. The essential elements of these systems are: flexible shafts, rigid disks, bearings, and a gear pair. The shaft is modelled through beam elements with 2 nodes and 6 d.o.f.s. by each node. These Finites elements include the effects of torsion, bending and tension-compression. The generalised displacement of the j^{th} node is given by:

$$(11)\qquad \{q\}^T = \{u_j, v_j, w_j, \varphi_j, \psi_j, \theta_j\},$$

where (u_j, ψ_j) and (v_j, φ_j) are the beam bending in the $(\overrightarrow{e_x}, \overrightarrow{e_y})$ plane and in the $(\overrightarrow{e_y}, \overrightarrow{e_z})$ plane respectively, w_j and θ_j are the degrees of freedom associated with the axial and torsion deformations respectively.

The outer races of the Bearings are fixed in the rigid support (logging) and the inner races are press-fitted on the rotating shafts and gyroscopic effects are neglected. The dynamic equation of the overall system, which includes all shafts transmission elements and bearings, can be expressed in a general form as follows:

$$[M_{tot}]\{\ddot{q}\} + [C]\{\dot{q}\} + [K_{tot}(t)]\{q\} = \{F_0(t)\} + \sum_{i=1}^{N_{pal}} \{F_{pal}(t,q)\}, \tag{12}$$

where $[M_{tot}]$, $[C]$ and $[K_{tot}(t)]$ represent the global mass, damping and stiffness matrices depending on the transmission system respectively.

$\{F_0(t)\}$ is the vector of external force and $\sum_{i=1}^{N_{pal}} \{F_{pal}(t,q)\}$ represents the forces exerted by all ball bearings on their inner races fixed on the shafts. F_{pal} expression is given by equation (10).

In this study gear transmission error and ball bearing waviness are considered as excitation sources of the system. The gear meshing process is modelled with a time-varying stiffness matrix [13], [14]:

$$[k_g(t)] = k(t)[G], \tag{13}$$

where, matrix $[G]$ is derived from geometric characteristics of the gear pair and $k(t)$ is the periodic mesh stiffness. Trapezoidal waves are used for helical gears, to approximate the mesh stiffness alternating between n and $n+1$ pairs of teeth in contact. In this study, $k(t)$ is specified by a mean value $\bar{k}$ and varying part $k_v(t)$, periodic at mesh frequency $F_{eng} = Z_p.f_i$, where Z_p and f_i represent the number of teeth on the pinion and the input shaft rotational frequency [13] respectively. Equation (13) can be changed into the following form:

$$[k_g(t)] = \left(\bar{k} + k_v(t)\right)[G]. \tag{14}$$

The global stiffness matrix $[K_{tot}(t)]$ inserting equation (14) into the governing equation (12) can be written as:

$$[K_{tot}(t)] = \left[\bar{K}_{tot}\right] + k_v(t)[G], \tag{15}$$

where $\left[\bar{K}_{tot}\right]$ is the stiffness matrix represented by the mean value of the total transmission system [15].

4. Numerical simulations

The system investigated in this paper is shown in Fig. 4 and represents a single stage gear that consists of a helical gears pair mounted on two flexible shafts and supported by 4 angular ball bearings. The main characteristics of each component are presented in Table 1. We are interested to analyze vibrations generated by a gear coupled to two shafts bearing system in the presence of faults.

The equation of motion (12) is solved with respect to the algorithm described in Fig. 3 to obtain the dynamic response of the gear-bearing system [11]. First, the natural frequencies and the corresponding system mode shapes

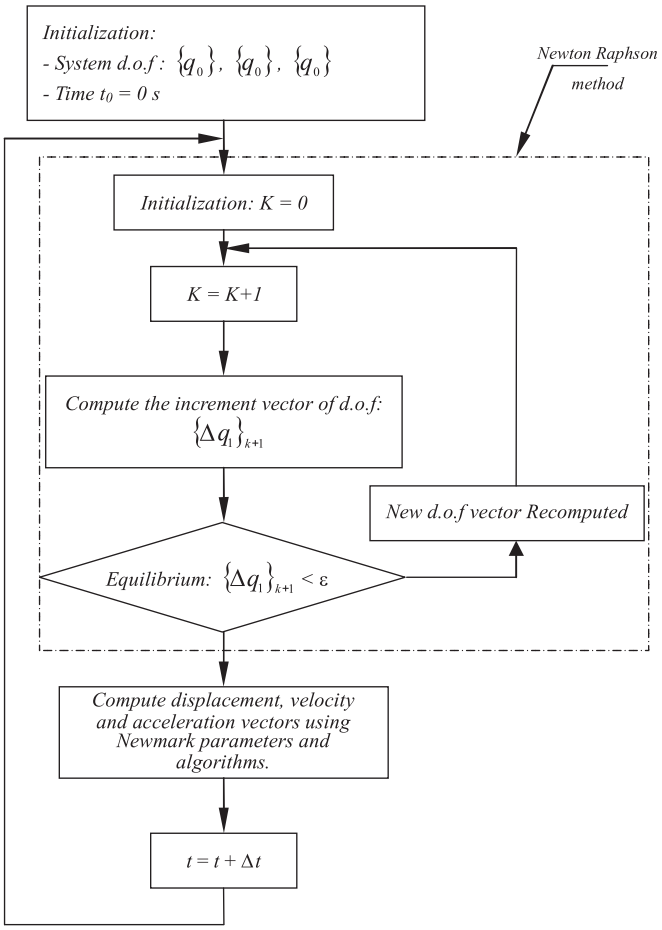

Fig. 3. Numerical procedures to calculate the nodal dynamic response

Table 1. Main characteristics of the model

Helical Gear Pair Characteristics	
Number of teeth (pinion, gear)	26,157
Normal module m_0 (m)	$4\ 10^{-3}$
Pressure angle (deg)	20
Face width (m)	$4\ 10^{-2}$
Base helix angle (deg)	30
Ball Bearing Characteristics	
Number of ball	10
Ball diameter (m)	$12{,}7\ 10^{-3}$
Pitch diameter (m)	$70\ 10^{-3}$
Inner and outer race curvature radius (m)	$6{,}572\ 10^{-3}$
contact angle (deg)	10,2
Races waviness amplitude (m)	5.10^{-6}
Ball waviness amplitude (m)	10^{-6}
System Characteristics	
Modal damping coefficient	0.02
Shafts length (m)	$850\ 10^{-3}$

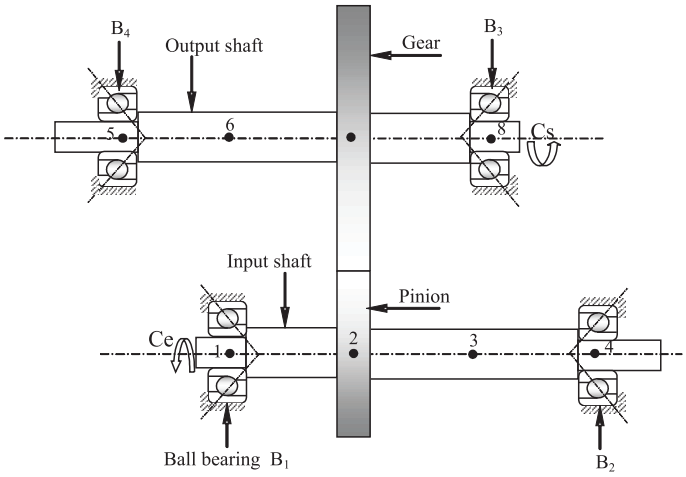

Fig. 4. Schematic of the studied system

are computed. Then, the dynamic equation is projected in the chosen modal basis and a constant modal damping coefficient is used for all considered modes. The Newmark method coupled with the iterative Newton Raphson method, which resolve the system equilibrium at each step, are used to compute the system temporal response. The dynamic responses are therefore obtained by modal recombination.

4.1. Natural frequencies and vibration modes

The eigenvalue problem of the studied system associated, for the time invariant case, with equation of motion (12) is:

$$\left[\bar{K}_{tot}\right]\{\Phi_i\} = \omega_i^2\left[M_{tot}\right]\{\Phi_i\}, \tag{16}$$

where ω_i and $\{\Phi_i\}$ are the natural frequencies and vibration modes respectively.

Modal characteristics of helical gear pair mounted on two flexible shafts and supported by 4 angular ball bearings are recovered from the finite element analysis model. The first 9 natural frequencies associated to the studied system are recapitulated in Table 2. We note the presence of a rigid-body mode corresponding to the system rotation, and the presence of 7 frequencies that can be excited in the band operating frequency of the system [0–1200 Hz].

Table 2. Natural frequencies of the system

Mode number	Natural frequency (Hz)
1	0
2	89
3	99.5
4	171
5	180
6	386
7	563
8	720
9	1290

4.2. Dynamic response analysis

A 2% viscous modal damping ratio is considered for all numerical results proposed in this paper. A constant input torque equal to 300 Nm and an input shaft rotation is equal to 20 Hz are applied. The reduction rapport is equal to 0.165 (teeth number of pinion and gear are 26 and 157 respectively). The time-varying mesh stiffness and forces exerted by all ball bearings are considered as the excitation source of the gear transmission system. The ball and the cage frequencies are computed from rolling without slipping conditions.

Figure 5a represents the spectrum of the radial displacement of the ball bearing B_1. We note the presence of the gear frequency (Feng = 520 Hz). The power spectrum response is examined by zooming at 0–35 Hz (Fig. 5b) in order to identify the frequencies corresponding to the rolling elements. Note the existence of the input and output bearings cage frequencies ($fcB_1 = 1.35$ Hz, $fcB_2 = 8.3$ Hz) and their harmonics.

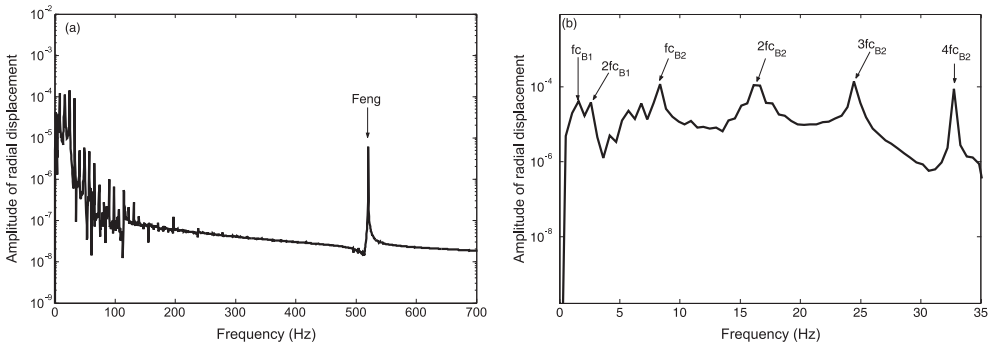

Fig. 5. Spectrum displacement of the ball bearing B_1 observed at node 1

A gear mesh system having reduction rapport equal to 1 is considered for the rest of the investigation, where the number of teeth is equal to 18. This configuration allows reducing the number of frequency components. In this case, cage frequencies (fc_1, fc_2) and ball passage frequencies ($Z.fc_1$, $Z.fc_2$) of each bearing will be equal.

Simulations were performed in order to illustrate the effect of the ball bearing on the gear transmission dynamic response, for two types of formulations. A comparative study, given by Fig. 6, is realized between an instantaneous ball bearings effect formulation (presented model) and a constant radial bearings stiffness matrix formulation (spring bearing model). Figure 6 shows the spectrum of radial displacement for both modelling conducts to the gear mesh frequency presence due to the gear stiffness variation in time. It is noticed in addition to the gear mesh frequency the presence of the modulation between gear mesh (Feng) and cage frequencies (fc) when we take in account the non-linear bearing effect. A remarkable underestimation of the global level of vibration is performed by considering a spring bearing.

The time-domain response is computed for the excitation described above, in several d.o.f. of the system. Radial and axial efforts on the roller bearing are generated by the existence of a helical gear. Figure 7 shows the relative contribution of the excitation source in terms of radial effort observed on ball bearing B_1. The spectrum presents significant amplitudes relative to the gear mesh frequency peak and the ball passage frequency (Z.fc) and its harmonics. It is also noticed, the presence of peaks corresponding to the modulation between gear mesh and ball passage frequencies (Feng $\pm$ Z.fc).

Figure 8 displays the root mean square (RMS) of the radial effort exerted by the input bearing B_1 on the gear system against the gear mesh

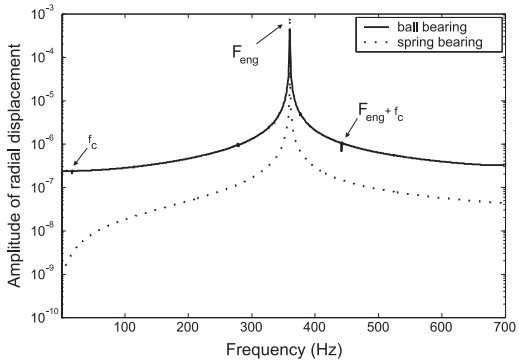

Fig. 6. Spectrum of radial displacement for both modelling (with spring bearing and ball bearing B_1) observed at node 1

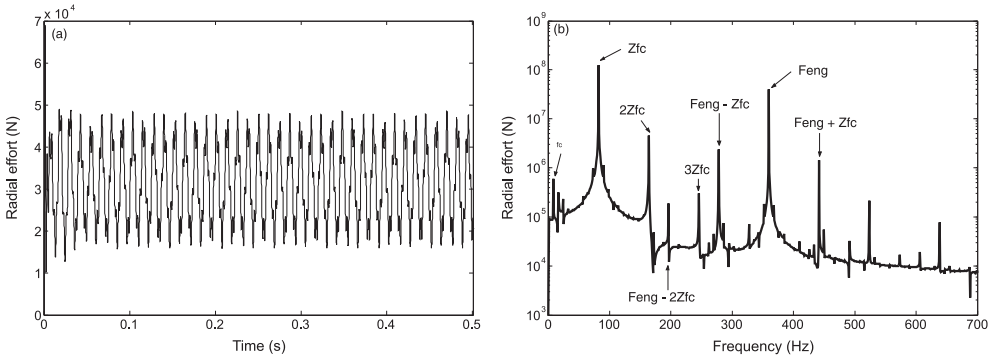

Fig. 7. (a) radial effort exerted by the input bearing B_1 with time, (b) Fourier Transform of the radial effort exerted by the input bearing B_1

frequency. The result is relative to the frequency range of 50–600 Hz. It shows multiple parametric resonances corresponding to the excitation of critical modes.

4.3. Impact of waviness on dynamic response

The introduction of inner race waviness conducts to the apparition of the waviness frequency varying with respect to waviness order and waviness amplitude. The simulation is performed at a gear mesh frequency Feng = 360 Hz. A comparative analysis of the evolution of the ball bearing B1 radial displacement with and without defect is made. Figure 9 shows an amplitude modulation of the gear mesh signal with inner race waviness defect signal (inner race waviness order $l = Z - 1$), this is the result on the corresponding spectrum in two sideband frequency components around the frequency gear mesh (Feng

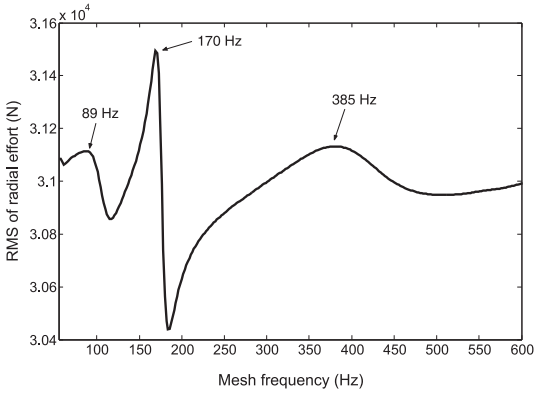

Fig. 8. RMS of radial effort exerted by the input bearing B_1 versus mesh frequency

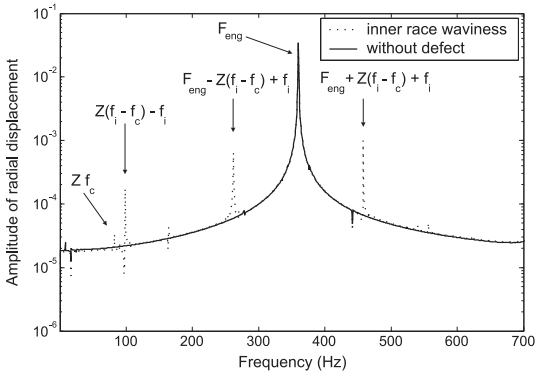

Fig. 9. Frequencies displacement response of ball bearing B_1 with and without inner race waviness (waviness order $l = 9$)

$\pm$ fd). We also note the presence of the defect frequency $fd = Z.(fi - fc) - fi$.

The simulation results are presented for inner race waviness order $l = 9, 10$ and 11 in order to illustrate the effect of waviness order on the dynamic behaviour system. The presence of ball bearing defect is revealed in Fig. 10a, b and c by the emergence of three characteristics frequencies: gear mesh frequency, cage frequency and ball passage frequency. The apparition of the defect frequency fd, and a modulation between the gear mesh frequency and defect frequency (Feng $\pm$ fd) is also noted. The defect frequency appears at $Z.(fi - fc)$ for a waviness number equal to 10 (Fig. 10b). However, it becomes visible at $Z.(fi - fc) + fc$ for $l = 11$ (Fig. 10c).

The last part of the section is devoted to study the effect of rolling element defect. The radial and axial displacement frequency response of the

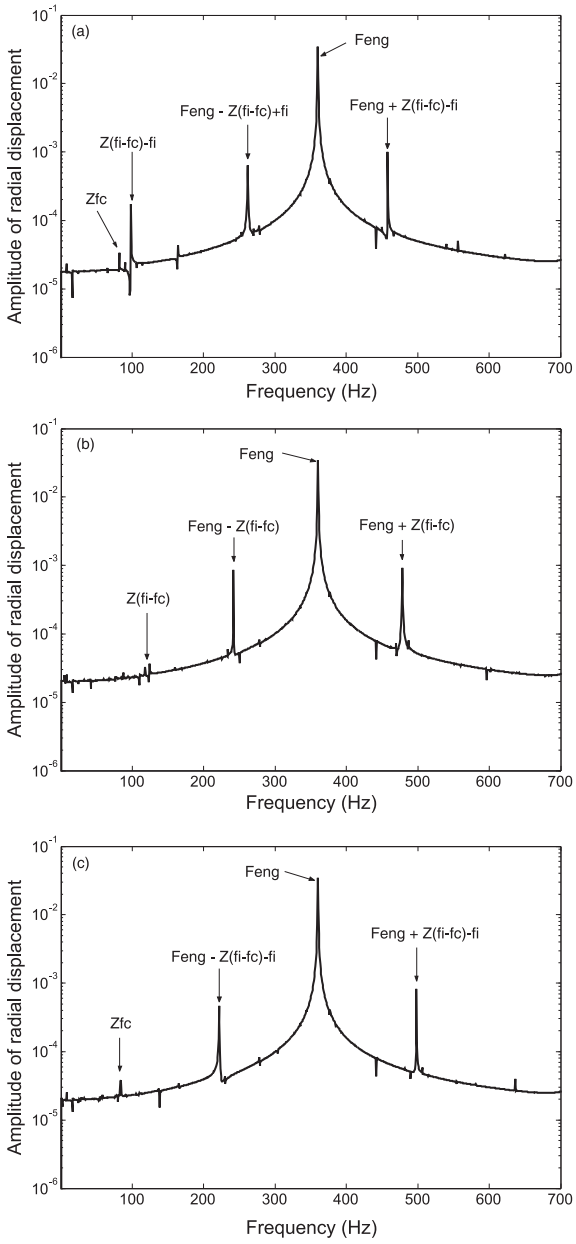

Fig. 10. Frequencies displacement response of ball bearing B_1 with inner race waviness (a): waviness order $l = 9$, (b): waviness order $l = 10$, (c): waviness order $l = 11$

ball bearing B_1 are illustrated in Figs 11a, b. The presented results are relative to a bearing having ball waviness. The frequency spectra for the computed response of the system show the presence of peaks corresponding to the gear mesh frequency, the ball passage frequency and the waviness frequency. There is also a modulation between the gear mesh and the defect frequencies. The defect frequencies depend to the order of ball waviness and $fd = 2fb$ or 4fb respectively for a number of waviness equal to 2 or 4. Figures 12a, b illustrate the horizontal and the vertical displacement responses of rolling bearing inner race centre located on the nodes 1 (B_1) and 5 (B_4). The figures show, when the balls have waviness, the orbit amplitude and the fluctuation are more important.

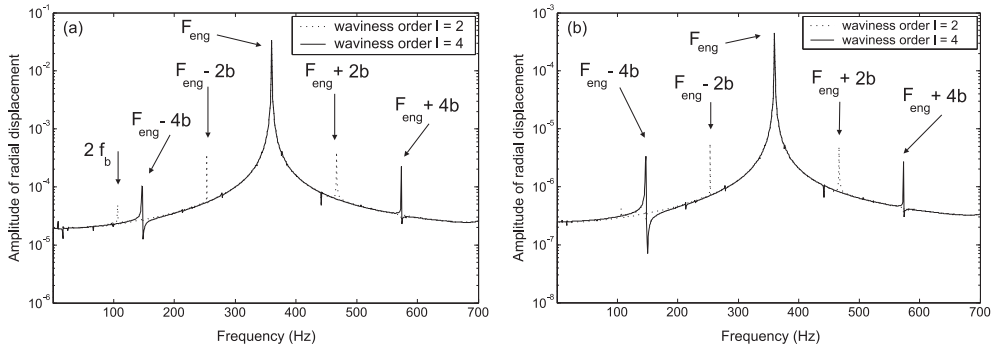

Fig. 11. Frequencies displacement response of ball bearing B_1 with ball waviness (a): amplitude of radial displacement, (b): amplitude of axial displacement

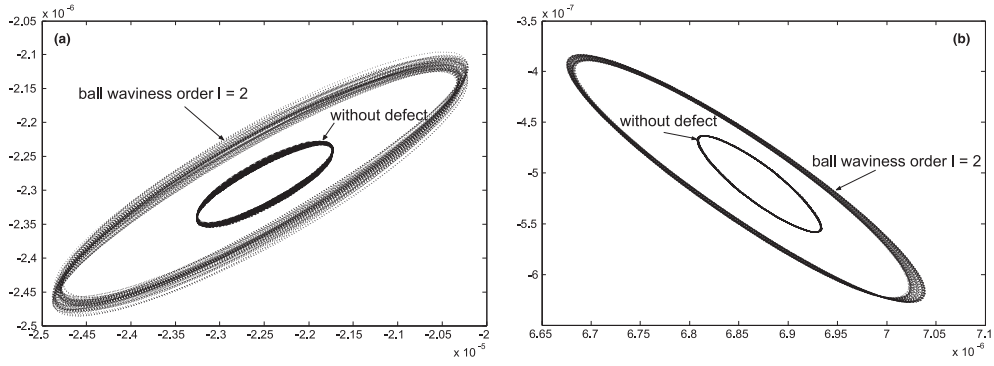

Fig. 12. Displacement orbit response with and without ball waviness observed at (a): ball bearing B_1, (b): ball bearing B_4

5. Conclusion

In this paper, the vibration and the associated dynamic behaviour of a helical gear supported by ball bearing is numerically studied. A finite element formulation is developed for simulating the dynamic interaction of gear and bearing in presence of faults. Time-varying gear-meshing process is considered and Hertzian contact theory is applied to compute the elastic deflection and the non linear contact force exerted by the totality bearings balls on the input and output shafts. Numerical simulations are carried out to investigate the effects of these excitation sources on the dynamic response of the gear transmission system. The vibration spectra are dominated by the vibration at the gear mesh frequency coming from the mesh stiffness variation, the cage frequency where the origin is the bearing rotation and the ball passage frequency as a result of the bearing stiffness variation. The influence of the Ball bearing waviness on the system transmission dynamic behaviour is also studied. The waviness, defined as the difference between the real and the manufactured contact surfaces, generates excessive vibrations depending on the waviness type, the location and the order. Frequencies responses show the presence of waviness frequencies and their modulation with gear mesh and the ball passage frequencies. The presented simulated signals with well-defined characteristics can be very valuable to develop diagnostic and prognostic techniques for rolling element bearings in real systems.

REFERENCES

[1] Lim, T. C., R. Singh. Vibration Transmission through Rolling Element Bearings. Part I: Bearing Stiffness Formulation. *Journal of Sound and Vibration,* **139** (1990), No. 2, 179–199.

[2] Lim, T. C., R. Singh. Vibration Transmission through Rolling Element Bearings. Part II: System Studies. *Journal of Sound and Vibration,* **139** (1990), No. 2, 201–225.

[3] Jang, G., S. W. Jeang. Nonlinear Excitation Model of Ball Bearing Waviness in a Rigid Rotor Supported by Two or More Ball Bearings Considering Five Degrees of Freedom. *Trans of ASME, Journal of Tribology*, **124** (2002), 82–90.

[4] Jang, G., S. W. Jeang. Vibration Analysis of a Rotating System due to the Effect of Ball bearing Waviness. *Journal of Sound and Vibration*, **269** (2004), No. 3–5, 709–726.

[5] Harsha, S. P. Nonlinear Dynamic Analysis of a High-speed Rotor Supported by Rolling Element Bearings. *Journal of Sound and Vibration*, **290** (2006), No. 1–2, 65–100.

[6] Kankar, P. K., S. P. Harsha, P. Kumar, S. C. Sharma. Fault Diagnosis of a Rotor Bearing System using Response Surface Method. *European Journal of Mechanics A/Solids,* **28** (2009), No. 4, 841–857.

[7] Rafsanjania, A., S. Abbasiona, A. Farshidianfarb, H. Moeenfardc. Nonlinear Dynamic Modelling of Surface Defects in Rolling Element Bearing Systems. *Journal of Sound and Vibration,* **319** (2009), No. 3–5, 1150–1174.

[8] Sawalhi, N., R. B. Randall. Simulating Gear and Bearing Interactions in the Presence of Faults. Part I. The Combined Gear Bearing Dynamic Model and the Simulation of Localised Bearing Faults. *Mechanical Systems and Signal Processing,* **22** (2008), No. 8, 1924–1951.

[9] Abbes, M. S., S. Bouaziz, F. Chaari, M. Maatar, M. Haddar. An Acoustic-structural Interaction Modelling for the Evaluation of a Gearbox Radiated Noise. *International Journal of Mechanical Sciences,* **50** (2008), No. 3, 569–577.

[10] Walha, L. T. Fakhfakh, M. Haddar. Nonlinear Dynamics of a Two-stage Gear System with Mesh Stiffness Fluctuation, Bearing Flexibility and Backlash. *Mechanism and Machine Theory,* **44** (2009), No. 5, 1058–1069.

[11] Abbes, M. S., T. Hentati, M. Maatar, T. Fakhfakh, M. Haddar. Dynamic Behaviour of a Rotor Supported by Angular Ball Bearings. *Diagnostyk*a, **51** (2009), No. 3, 3–8.

[12] Wensing, J. A. On the Dynamics of Ball Bearings, Ph.D. Thesis, University of Twente, Enschede, The Netherlands, 1998.

[13] Lin, J., R. G. Parker. Mesh Stiffness Variation Instabilities in Two Stage Gear Systems. *Journal of Vibration and Acoustics,* **124** (2002), No. 1, 68–76.

[14] Ajmi, M., P. Velex. A Model for Simulating the Quasi-statistic and Dynamic Behaviour of Solid wide-face Spur and Helical Gears. *Mechanism and Machine Theory,* **40** (2005), No. 2, 173-90.

[15] Abbes, M. S., M. Trigui, F. Chaari, T. Fakhfakh, M. Haddar. Dynamic Behaviour Modelling of a Flexible Gear System by the Elastic Foundation Theory in Presence of Defects. *European Journal of Mechanics A/Solids,* **29** (2010), No. 5, 887–896.

Nomenclature

D_i inner raceway groove diameter
D_m pitch diameter
D_0 outer raceway groove diameter
D_b ball diameter
r_0 outer race curvature radius
r_i inner race curvature radius
P_d diametrical clearance
α_0 unloaded contact angle
α_j loaded contact angle
Z rolling element number

C_r rolling element centre
O_2 geometric inner race centre
O_1 geometric outer race centre
ψ_j rolling element angular position
K_p Hertz contact constant
a_1, R_1 axial and radial outer race curvature centre
p_{ij}, p_{oj} radial outer race waviness and axial outer race waviness
q_{ij}, q_{oj} radial inner race waviness and axial inner race waviness
w_j ball waviness
$A_{bl}, alpha_b^l$ ball waviness amplitude and initial phase
A_{il}, B_{il} radial and axial inner race waviness amplitude
α_i^l, β_i^l radial and axial inner race waviness initial phase
A_{ol}, B_{ol} radial and axial outer race waviness amplitude
α_o^l, β_o^l radial and axial outer race waviness initial phase
f_b ball rotating frequency
f_o outer race rotating frequency
f_i inner race (shaft) rotating frequency
f_c cage rotating frequency
l waviness order
Δ_j elastic deformation of the jth rolling element
d_0 unloaded relative distance between the inner and the outer raceway groove curvature centers O_{1j} and O_{2j}
$d(\psi_j)$ loaded relative distance between the inner and the outer raceway groove curvature centers O_{1j} and O_{2j}
$\Delta_{rj}^*, \Delta_{zj}^*$ radial and axial elastic deformations
$[K_g(t)]$time varying stiffness matrix
$k\,(\mathrm{t})$ periodic stiffness function
$k_v\ (t)$ varying part of periodic mesh stiffness
$\overline{k}$ mean value of periodic mesh stiffness
$[G]$ form matrix
$[M_{tot}]$, $[C]$ global mass and damping matrices
$[K_{tot}\,(t)]$ global stiffness matrix depending on time
$\{F_0\}$ static external force
$\sum_{i=1}^{N_{pal}} \{F_{pal}\}$ forces exerted by ball bearings on the inner race
$\Re_1$ global coordinate frame
$\Re_2$ radial coordinate frame associated to the cage motion
ω_i natural frequencies
$\phi_i$eigenvector matrix
$\{q\}, \{\dot{q}\}, \{\ddot{q}\}$ displacement, speed and acceleration degrees of freedom vector